Composites: Part B 42 (2011) 771–780

Contents lists available at ScienceDirect

Composites: Part B

journal homepage: www.elsevier.com/locate/compositesb

Finite element simulation of ceramic/composite armor under ballistic impact

S. Feli *, M.R. Asgari

Department of Mechanical Engineering, Razi University, P.O. Box: 67149, Kermanshah, IR of Iran

ARTICLE INFO

Article history:
Received 25 September 2010
Received in revised form 2 December 2010
Accepted 23 January 2011
Available online 31 January 2011

Keywords:
A. Fibers
B. Impact behavior
C. Finite element analysis (FEA)
Ceramic/composite armor

ABSTRACT

In this paper, based on LS-Dyna code, a new finite element (FE) simulation of the ballistic perforation of the ceramic/composite targets, which impacted by cylindrical tungsten projectiles, has been presented. Research on this method has been conducted by a few research groups in recent years. The ceramic material, which is the front plate, has been made of Alumina 99.5% and composite back-up plate composed of Twaron fibers. The 2-dimensional (2D), axi-symmetric, dynamic-explicit, Lagrangian model has been considered in this simulation. The Johnson–Cook, Johnson–Holmquist and Composite-Damage materials behaviors have been used for projectile, ceramic and composite materials respectively. The brittle fracture and fragmentation of ceramic conoid, the failure criteria based on fracture of fibers or matrixes of composite materials and erosion or flattening of projectile during perforation have been considered. The residual velocity and perforation time has been obtained and compared with the available analytical models. The results show that when the ceramic is impacted by a projectile, a fragmented ceramic conoid breaks from ceramic tile and the semi-angle of ceramic conoid with increasing initial velocity decreases. Furthermore, the dishing of composite layers at high impact velocities and the delamination of layers near the ballistic limit velocity decrease.

1. Introduction

The non-metallic materials, such as ceramics and composites, have been increasingly incorporated into more efficient lightweight armor. Mixed armors made of ceramic tiles and a composite laminated plate, seem to form a very efficient shield against low and high velocity impact, since they combine low density, high hardness, high rigidity and strength in compression of ceramic with the lightweight and ductility of composite laminated. The two-layer ceramic/composite armor has been used widely in light weight vehicles, personal armors, helicopter and airplane and in airplane protection. When a projectile impact onto ceramic/composite, the projectile is first eroded or flatted by the hard ceramic and the reflected tensile wave breaks the ceramic in tension. The backing composite layer deforms to absorb the remaining kinetic energy of the projectile.

There are many studies on the ballistic impact behavior of composite materials. The earliest efforts were those of Roylance [1] on biaxial fabrics. They implemented a dynamic form of FE analysis and obtained many behavioral features seen in experiments.

Zhu et al. [2] investigated the penetration resistance of Kevlar laminates under impact of projectile by analytical and experimental methods.

Wen [3] presented simple relationships for predicting the perforation of monolithic fabric-reinforced plastic (FRP) laminates, struck normally by projectiles, with different nose shapes over a wide range of impact velocities.

Gu [4] presented an analytical model to calculate decrease of the kinetic energy and residual velocity of projectile penetrating targets composed of multi-layered planar woven fabrics. The strain-rate effect and the rate-dependent properties of fibers have been considered in this model.

Cottrell et al. [5] purposed a method based on, erosive techniques, of adaptive remeshing and meshless particle methods for long-rod penetration in ceramics. These methods are pursued in order to provide additional tools for the numerical model to enhance the understanding of penetration processes that occur at various impact velocities, such as those of radial flow of the projectile and of intermittent and asymmetrical penetration.

Fawaz et al. [6] investigated the oblique ballistic impact on composite armor. They have shown that the projectile erosion during oblique impact is slightly greater than that of normal impact.

Gu and Xu [7] investigated the ballistic perforation of 4-step 3-dimensional (3D) braided Twaron/epoxy composites, which were subjected to impact by conically cylindrical steel projectile. The residual velocities of projectile perforated composites target at various strike velocities were measured and compared with that from FE code of LS-Dyna.

Mamivand and Liaghat [8] developed an analytical model for the ballistic behavior of 2-dimensional (2D) woven fabric composites. The penetration process of cylindrical projectile based on the conservation of momentum and wave theory was simulated

* Corresponding author. Tel.: +98 (831) 4274535/9; fax: +98 (831) 4274542.
E-mail address: Felisaeid@gmail.com (S. Feli).

1359-8368/$ - see front matter © 2011 Elsevier Ltd. All rights reserved.
doi:10.1016/j.compositesb.2011.01.024

and the effect of target dimensions on its ballistic performance was also been studied.

Sabouri and Liaghat [9] developed some modification formulas for strain energy and static and dynamic response of fiber-metal laminates.

The analysis of two-layer ceramic–composite armor which is investigated in this paper is complex and hence has not been treated numerically by previous researchers. Chocron–Galvez [10] analytical and numerical models, Shokrieh and Javadpour [11] numerical model and Feli et al. [12] analytical model, have been developed to describe this system so far.

Chocron–Galvez [10] analytical model has been developed to describe projectile impacting a ceramic backed by a composite plate. The perforation process has been divided into three phases. In this model the residual velocity and length of the projectile and projectile time-history has been compared with the numerical simulation. The numerical simulation has not been explained clearly in this paper.

Shokrieh and Javadpour [11], used Ansys/LS-Dyna software, to determined the ballistic limit velocity of boron carbide ceramic backed by Kevlar 49 fiber composite material. In this simulation the equivalent mechanical properties of the laminate composite and ceramic has been used. The Heterington [12] equation (optimum thickness of layers) has been verified for constant thickness of the armor.

Feli et al. [13] developed the Chocron–Galvez [10] analytical model. In this model for describing the fragmented ceramic conoid, the Zaera–Galvez [14] analytical model has been used. For modeling the back-up woven-fabric material and deformation of yarns during perforation, the kinetic and strain energy of yarns has been determined.

In the previous numerical methods mentioned above, for simulation of the ceramic and composite materials, the equivalent mechanical properties or material behavior has been used. Neither the brittle fracture or erosion of ceramic under high pressure and strain rate, fragmentation and large deformation of ceramic during perforation has been considered nor the failure criteria based on fracture of fibers or matrixes of composite material. Furthermore, the effects of strain rate and work hardening on material behavior of projectile and erosion or flattening of projectile during perforation has also been neglected.

The purpose of this paper is to demonstrate a new technique for FE simulation, based on LS-Dyna FE code, for normal penetration of cylindrical projectiles onto the ceramic–composite targets. In this model the above mention assumes is modified. For describing the fragmentation of ceramic front plate the Johnson–Holmquist continuum based plasticity model is used. In this model the brittle failure, effects of high pressure and strain rate and large deformation of ceramic material under high velocity impact is considered. For modeling the composite material the Composite-Damage model in LS-Dyna FE code is chosen, which contains three failure criteria including fiber fracture, matrix cracking or compressive failure. Also the effects of work hardening, strain rate, erosion, and temperature is considered in the tungsten projectile material. Furthermore, the erosion model including failure in material models and deletes the elements from calculations is used. The values of residual velocity and perforation time are compared with the results of other researchers. In addition, the performance of ceramic/composite armor subjected to ballistic impact is investigated.

2. Finite element modeling description

2.1. Projectile specifications

The cylindrical tungsten projectile of 10 mm in diameter, 30 mm length and 41.7 g in mass has been used in FE simulation. The Johnson–Cook material behavior equation [15], which considers the effects of work hardening, strain rate and temperature in mechanical behavior of projectile, has been chosen:

$$\sigma(\varepsilon_p, \dot{\varepsilon}_p, T) = (A + B\varepsilon_p^n)(1 + C\ln\dot{\varepsilon}_p^*)(1 - T^{*m}) \tag{1}$$

In the above equation, A, B, C, n, m are the Johnson–Cook material behavior coefficients and:

$$\dot{\varepsilon}_p^* = \frac{\dot{\varepsilon}_p}{\dot{\varepsilon}_{p0}} \quad T^* = \frac{T - T_0}{T_m - T_0} \tag{2}$$

where ε_p is the plastic strain, $\dot{\varepsilon}_p$ the equivalent strain rate, $\dot{\varepsilon}_0$ reference strain rate, T current temperature, T_0 room temperature and T_m is the melting temperature.

To characterize the plastic material behavior at high pressures, typical for highly dynamic processes, the relation between the hydrostatic pressure, the local density (or specific volume), and local specific energy has been used. This relation is known as equation of state (EOS). The most commonly used reference curve to establish the Mie–Gruneisen EOS for solid materials is the shock Hugoniot and is defined in the LS-Dyna code as [16]:

$$P = \frac{\rho_0 c_0^2 \mu[1 + (1 - \frac{\gamma_0}{2})\mu - \frac{a}{2}\mu^2]}{[1 - (S_1 - 1)\mu - S_2\frac{\mu^2}{\mu+1} - S_3\frac{\mu^3}{(\mu+1)^2}]^2} + (\gamma_0 + a\mu)E \tag{3}$$

In the Eq. (3), P is Hydrostatic pressure, E internal energy, c_0 Elastic wave speed, S_1, S_2, S_3 Slope in U_s versus U_p diagram, γ_o and a Gruneisen coefficients, and μ is define as:

$$\mu = \frac{\rho}{\rho_0} - 1 = \frac{V_0}{V} - 1 \tag{4}$$

where ρ_0, V_0 the initial specific volume and density and ρ, V is the specific volume and density at the region that stress wave propagated. Material parameters for tungsten alloy used in the Johnson–Cook's model and the Mie–Gruneisen EOS have been presented in Table 1.

2.2. Ceramic and composite material specifications

The ceramic/composite target material has the total constant thickness 40 mm and radius 50 mm. The 2D, axi-symmetric model of projectile and ceramic–composite target has been shown in Fig. 1. A two-layer target has been made of alumina 99.5% with the density of 3700 kg/m^3 and thickness 20 mm as front plate backed with the Twaron composite (CT1000, 1680 dtex/1000f) with the total thickness of 20 mm. The composite back-up plate consists of 50 layers of Twaron fibers with the 0.4 mm of thickness as shown in Fig. 1.

Table 1
Material parameters for tungsten alloy used in Johnson–Cook's model and the Mie–Gruneisen equation of state [5].

Parameter	Notation	Value
Density (kg/m^3)	ρ	17,600
Young's Modulus (GPa)	E	314
Shear modulus (GPa)	G	122
Poison ratio	υ	0.29
Static yield stress (MPa)	A	1506
Strain hardening modulus (MPa)	B	177
Strain hardening exponent	n	0.12
Strain rate coefficient	C	0.016
Thermal softening exponent	m	1
Initial reference temperature (°K)	T_0	300
Melting temperature (°K)	T_m	1723
Slope in Us versus Up diagram	S	$S_1 = 1.23$ $S_2 = S_3 = 0$
Gruneisen coefficient	γ_0	1.54
Elastic wave speed (m/s)	C_0	4029

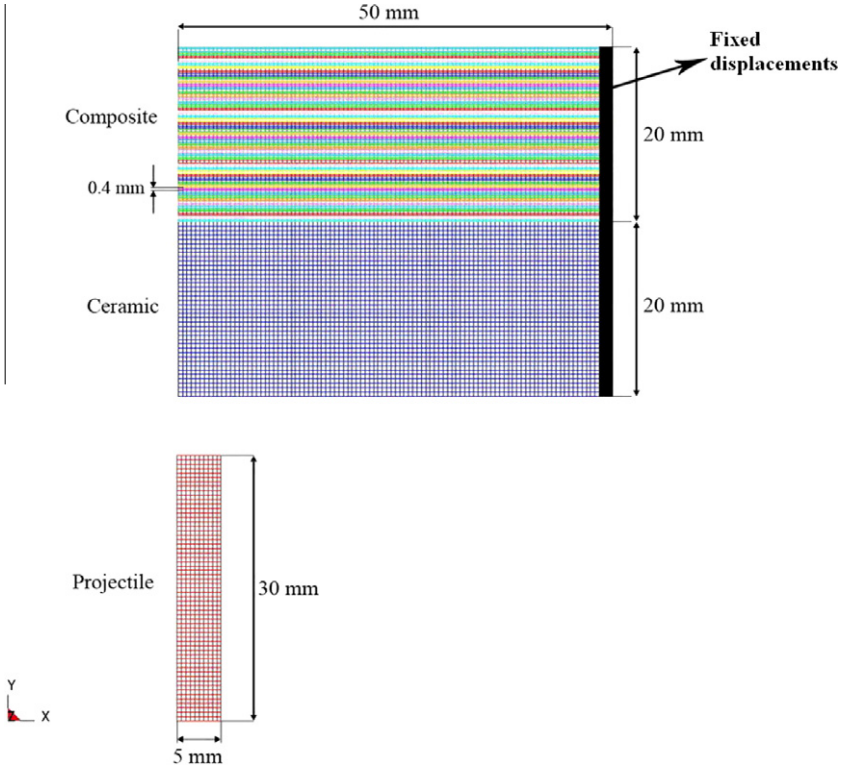

Fig. 1. The 2D axi-symmetric model of projectile and ceramic/composite target material.

2.2.1. Ceramic material specifications

The brittle failure model proposed by the Johnson–Holmquist [17] is well suited to the numerical constitutive modeling of brittle failure in ceramic material. The ceramic material is subjected to loading conditions that include high pressures, high strain rates and large deformations. The model is based upon a polynomial equation, which evaluates the current state of pressure as a function of the volumetric change [5]. The model includes a representation of the intact and fractured strength, a pressure–volume relationship that can include bulking and a damage model that transition from an intact state to a fractured state. The constitutive model comprises of three parts – strength, pressure and damage.

The intact and fractured ceramic material strengths are evaluated as nonlinear functions of normalized pressure (P^*), tensile strength (T^*) and the normalized total incremental strain rate [17]:

$$\sigma_i = \sigma_{HEL} A (P^* + T^*)^N (1 + C \ln \dot{\varepsilon}^*) \tag{5}$$

$$\sigma_f = \sigma_{HEL} B (P^*)^M (1 + C \ln \dot{\varepsilon}^*) \tag{6}$$

where σ_i and σ_f are intact and fractured ceramic strengths. σ_{HEL} is equivalent stress at the Hugoniot elastic limit and A, B, C are the Johnson–Holmquist parameters.

The initial hydrostatic pressure P is formed from the polynomial EOS:

$$P = K_1 \mu + K_2 \mu^2 + K_3 \mu^3 \tag{7}$$

where μ is given form Eq. (4).

For the transition stage, when the material is neither intact nor fully fractured the damaged material equivalent strength is formed as a combination of these two material strengths as [17]:

Table 2
Material parameters for Alumina 99.5% used in Johnson–Holmquist's model [17].

Parameter	Notation	Value
Density (kg/m^3)	ρ_0	3700
Shear modulus (GPa)	G	90.16
Intact strength coefficient	A	0.93
Fractured strength coefficient	B	0.31
Strain rate coefficient (s^{-1})	C	0
Fractured strength exponent	M	0.6
Intact strength exponent	N	0.6
Normalized maximum fractured strength	σ^f_{max}	0.2
Hugoniot elastic limit (MPa)	HEL	19,000
Pressure at Hugoniot elastic limit (MPa)	P_{HEL}	1460
Bulking factor	β	1
Elastic bulk modulus (MPa)	$K = K_1$	130,950
Coeff. For 2nd degree term in EOS (MPa)	K_2	0
Coeff. For 3rd degree term in EOS (MPa)	K_3	0
Damage coefficient	$D1$	0.005
Damage exponent	$D2$	1

Table 3
Mechanical properties of one of layer in fiber in Composite-Damage model [7].

Young's modulus (GPa)			Density (g/cm^3)ρ	Type	
E_1	E_2	E_3			
20.44	8.9	8.9	1.23	Twaron (CT1000, 1680 dtex/1000f)	
Shear modulus (GPa)			Poison ratio		
G_{12}	G_{13}	G_{23}	ν_{12}	ν_{13}	ν_{23}
1.64	1.64	3.03	0.31	0.31	0.49
Bulk modulus E_{bulk} (GPa)	Shear Strength S_{12}(GPa)	Longitudinal tensile strength S_1(GPa)	Transverse tensile strength S_2 (GPa)	Transverse compressive strength C_2 (GPa)	Non-linear parameters of shear stress α
20.4	0.34	1.145	0.13	0.65	0

Table 4
Material erosion parameters for Alumina 99.5%, tungsten alloy and Twaron used for erosive simulations.

Parameter	Notation	Tungsten projectile	Alumina 99.5%	Twaron fibers
Inelastic deactivation strain for erosive simulations (%)	*EPSP*1	80	6	3.4

$$\sigma = \sigma_i - D(\sigma_i - \sigma_f) \tag{8}$$

The damage term D is formed as the incrementally increasing function [17]:

$$D = \sum \frac{\Delta \bar{\varepsilon}^p}{\varepsilon_p^f + \frac{1}{3}G(\sigma_i - \sigma_f)} \tag{9}$$

The term ε_p^f is the originally proposed definition of the inelastic strain required to cause fracture of the material at a constant pressure:

$$\varepsilon_p^f = D1(P^* + T^*)^{D2} \tag{10}$$

which is evaluated as a function of the normalized pressure, the tensile strength and the two user prescribed damage constants $D1$ and $D2$.

The associated material parameters for the Johnson–Holmquist [17] material behavior used in LS-Dyna FE code are given in Table 2 [18].

2.2.2. Composite material specifications

The Composite material used as back-up plate is Twaron aramid filaments (type: Twaron CT1000, 3360 dtex/2000 f). The fiber volume content of the composite is 27%. Twaron is a kind of poly aramid fiber (poly paraphenylene terephthalamide, PPTA) similar to Kevlar. The specifications of Twaron aramid filaments are as: volume density: 1.44 g/cm^{3}Young's modulus: 65 GPa, failure stress: 2.8 GPa, failure strain: 3.4%.

The Material Type 22 (i.e. Composite-Damage Model) in LS-Dyna code has been chosen and the model is based on the Chang–Chang criterion, which contains three failure criteria [7].

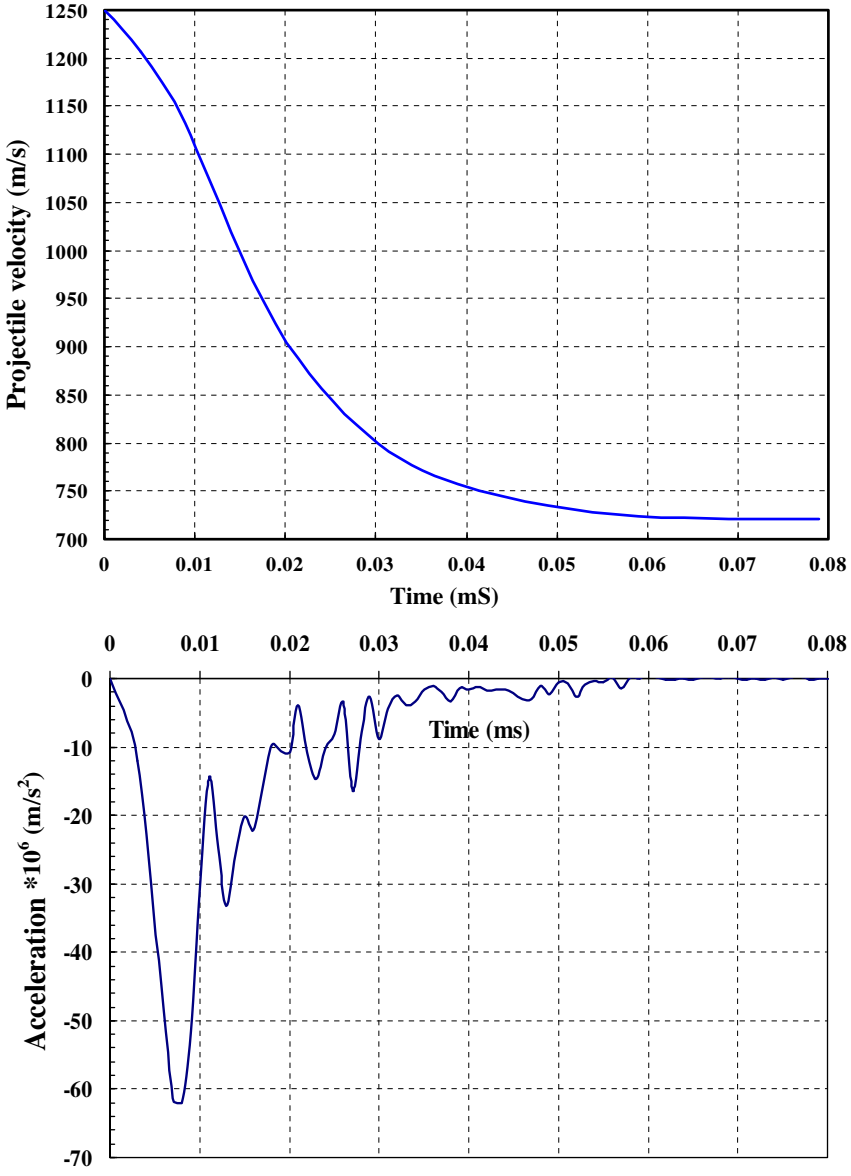

Fig. 2. Velocity and acceleration of projectile during perforation Projectile initial velocity: 1250 m/s.

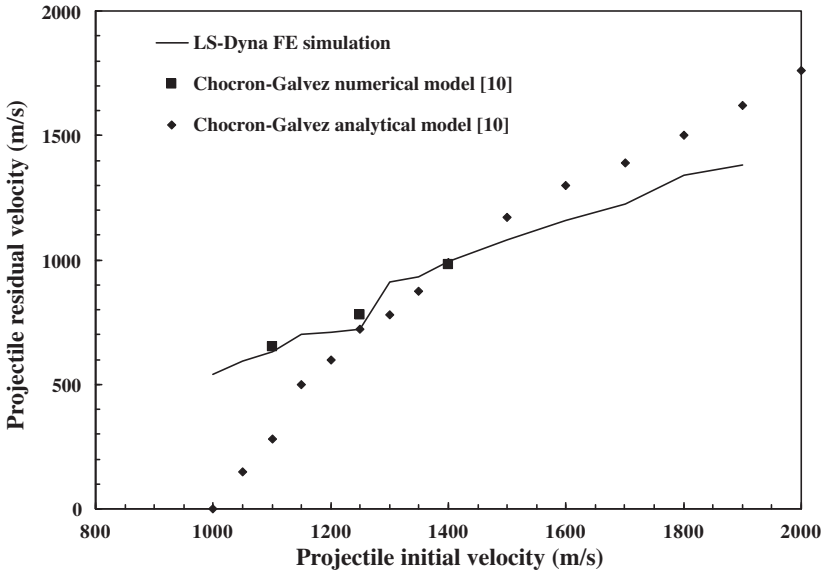

Fig. 3. Residual velocity versus initial velocity of projectile for tungsten projectile against ceramic/composite armor 20 mm/20 mm.

Failure of composite is deemed to occur when the combined stresses reach a critical value. It may result from fiber fracture, matrix cracking or compressive failure in accordance with the following rules:

2.2.2.1. Fiber fracture.

$$F_{fiber} = (\frac{\sigma_1}{S_1})^2 + \bar{\tau} \geqslant 1 \tag{11}$$

When fibers are fracture, the mechanical constants of composite E_1, E_2, G_{12}, v_1, v_2 are all set to zero.

2.2.2.2. Matrix cracking.

$$F_{matrix} = (\frac{\sigma_2}{S_2})^2 + \bar{\tau} \geqslant 1 \tag{12}$$

When matrixes are failure, E_2, G_{12}, v_1, v_2 are set to zero.

2.2.2.3. Compressive failure.

$$F_{comp} = (\frac{\sigma_2}{2S_{12}})^2 + \left[(\frac{C_2}{2S_{12}})^2 - 1\right]\frac{\sigma_2}{C_2} + \bar{\tau} \geqslant 1 \tag{13}$$

When compressive failure occurs, E_2, v_1, v_2 are set to zero.

In the above equations:

$$\bar{\tau} = \frac{\frac{\tau_{12}^2}{2G_{12}} + \frac{3}{4}\alpha\tau_{12}^4}{\frac{S_{12}^2}{2G_{12}} + \frac{3}{4}\alpha S_{12}^4} \tag{14}$$

S_1, S_2, S_{12} and C_2 are longitudinal tensile strength, transverse tensile strength, in-plane shear strength and transverse compressive strength, respectively.

The stress–strain relationship of the Composite-Damage model is as follows [7]:

$$\varepsilon_1 = \frac{1}{E_1}(\sigma_1 - v_1\sigma_2)\ \varepsilon_2 = \frac{1}{E_2}(\sigma_2 - v_2\sigma_1)2\ \varepsilon_{12} = \frac{1}{G_{12}}\tau_{12} + \alpha\tau_{12}^3 \tag{15}$$

Where ε_1, ε_2 are normal strain parallel to and perpendicular to fiber direction, respectively; ε_{12} is in-plane shear strain; σ_1, σ_2 and τ_{12} are stress corresponding to ε_1, ε_2 and ε_{12}, E_1, E_2 and G_{12} are Young's and shear modulus, v_1 and v_2 are Poisson's ratio in 1 and 2 direction; α is non-linear parameter of shear stress.

Fibers such as Kevlar and Twaron have anisotropic behavior; their thermo elastic properties along and transverse to the fiber axis are different. These fibers are considered to be transversely isotropic, and thus five independent constants are needed to describe their properties, namely E_{1f}, E_{2f}, G_{12f}, v_{12f} and G_{23f} [7]. The following expressions, due to Chamis [19], describe the elastic properties of a unidirectional lamina composed of anisotropic fibers in an isotropic matrix.

$$E_1 = E_{f1}V_f + E_mV_m, \quad E_2 = E_3 = \frac{E_m}{1 - V_f(1 - E_m/E_{f2})} \tag{16}$$

$$G_{12} = G_{13} = \frac{G_m}{1 - V_f(1 - G_m/G_{f12})},\ G_{23} = \frac{G_m}{1 - V_f(1 - G_m/G_{f23})} \tag{17}$$

$$v_{12} = v_{13} = v_{f12}V_f + v_mV_m,\ v_{23} = \frac{\frac{v_{f23}}{E_{f2}} + \frac{v_m}{E_m}}{\frac{V_f}{E_{f2}} + \frac{V_m}{E_m}} \tag{18}$$

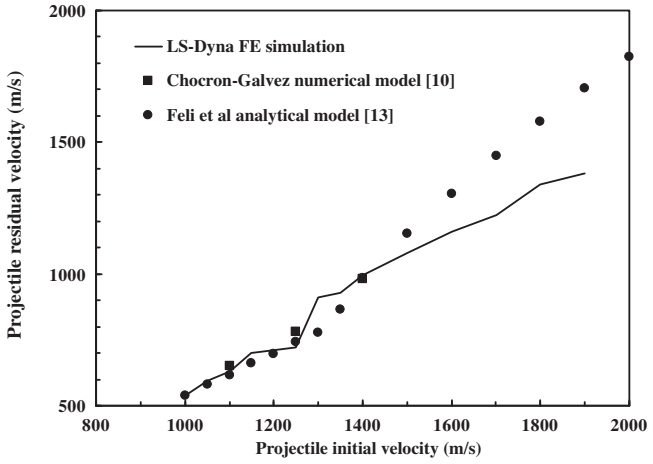

Fig. 4. Residual velocity versus initial velocity of projectile for tungsten projectile against ceramic/composite armor 20 mm/20 mm.

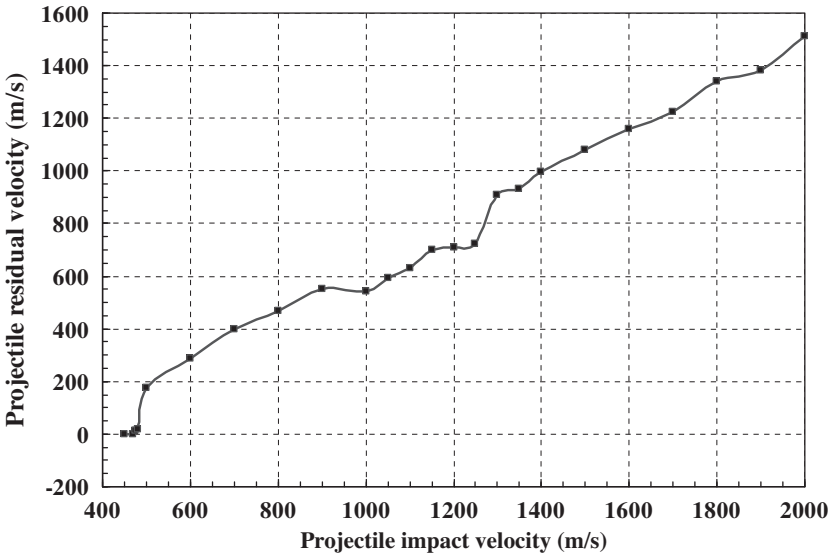

Fig. 5. Residual velocity versus initial velocity of projectile.

Table 5
Comparison of residual velocity computed by LS-Dyna FE code with Chocron–Galvez [10] and Shokrieh and Javadpour [11] numerical models.

Initial impact velocity (m/s)	470	475	480	500	600	800	900	1100	1250	1400
Residual velocity (m/s) LS-Dyna FE simulation	0	15	20	175	285	470	550	630	721	995
Residual velocity (m/s) Chocron–Galvez [10] numerical model	–	–	–	–	–	–	–	650	780	980
Residual velocity (m/s) Shokrieh and Javadpour numerical model [11]	–	–	–	–	–	–	–	–	770	960

In the above equations the index "*f*" refer to the fiber and "*m*" refer to matrix of composite material. From the mechanical properties of fibers and matrix, the elastic constants in above equations have been listed as in Table 3.

2.3. Material erosion model

The material behaviors models used in FE simulation, failed elements are not deleted from the computation. Thus the distortions due to large deformations of elements will drastically reduce the time step size needed to find a stable solution of the governing equations that will either stop computations or make them progress extremely slowly [20]. This is overcome by using the failure model Mat-add-erosion, regarding the material in an element to have failed with defined maximum principal strain and deleting the failed element from the calculation.

In this paper, the material erosion parameters for Alumina 99.5%, tungsten alloy and composite materials have been considered for erosive simulations. The parameters of material erosion are presented in Table 4.

2.4. Computerized model description

In the LS-Dyna FE code, the 2D, axi-symmetric, Lagrangian, dynamic-explicit and non-linear analysis has been utilized. The mesh scheme for the projectile, ceramic and composite layers has been shown in Fig. 1. A 2D axi-symmetric quadratic shell element with four nodes with *y* axes of symmetric has been used. The projectile and ceramic brick elements size is 0.5 mm × 0.5 mm and the every layer of composite material has the 0.5 mm × 0.2 mm element size.

The FE model considers realistic boundary conditions of the system during perforation. A zero values are imposed to the displacement in the *z*-direction and rotations in *x* and *y* direction for all the elements, also the edges of ceramic and composite layers is fixed. The initial impact velocity of projectile is considered as initial condition.

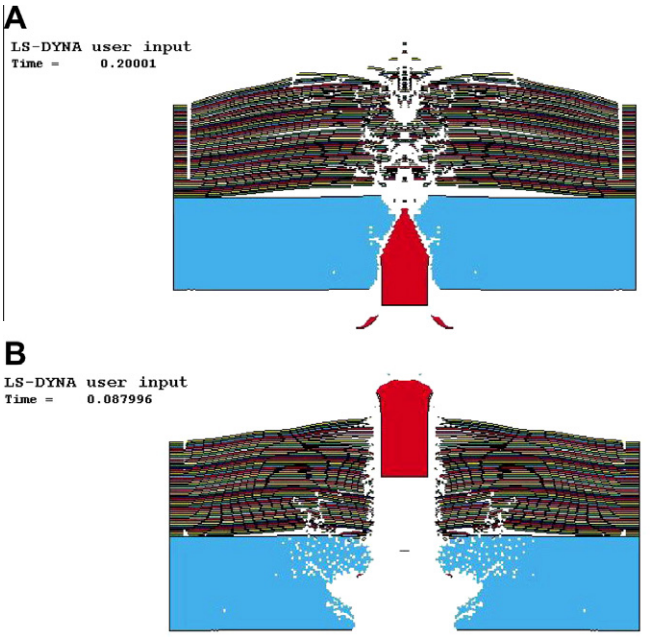

Fig. 6. The deformation of projectile, ceramic and composite material at A-Projectile initial velocity 470 m/s B-Projectile initial velocity = 900 m/s.

The "Contact_2D_automatic_surface_to_surface" option has been used for all contact surfaces during perforation process. The coefficient of friction between fabric layers is considered 0.3 [20],

also based on the simple experiment of Lim et al. [21] the coefficient of friction between projectile-ceramic and ceramic–composite surfaces is 0.28.

The "Constrained_tied_nodes_failure" option has been chosen to connect the interface between ceramic and composite layers. This option defines a tied node set with failure based on plastic strain. The specified nodes of ceramic and composite are tied together until the average plastic strain exceeds the specified value. When plastic strain of specified nodes is reached to failure plastic strain the nodes of elements that exceed the failure value are released to simulate the formation of a crack.

3. Results and discussion

3.1. Validation of FE model

The validity of the new FE simulation is assessed with the results available from the other references. The results of the simulation are compared with those from the Chocron–Galvez [10] analytical and numerical models, Feli et al. [13] analytical model and Shokrieh and Javadpour [11] numerical model. No reliable experimental results for valid new FE simulation were available.

Based on the references [22] and [7], specifications of Twaron and Kevlar 49 are approximately similar and therefore in this paper, results of FE simulation compared with the Chocron–Galvez [10] and Shokrieh and Javadpour [11] models that used Kevlar 49 (Dyneema) as back-up plate.

The velocity and acceleration of projectile during perforation computed by LS-Dyna FE code, at initial impact velocity 1250 m/s, has been shown in Fig. 2. It is clear that the perforation time is 79 μs and the residual projectile of projectile is 721 m/s. In the Chocron–Galvez [10] and Shokrieh and Javadpour [11] numerical models the perforation times have been computed as 69 μs and 320 μs respectively. In the Chocron–Galvez [10] numerical model a commercial hydrocode Autodyn-2D and in the Shokrieh and Javadpour [11] model the Ansys/LS-Dyna software have been used to simulate this projectile-target system, also the specifications of projectile and targets in this two models are same as this paper. Therefore, the perforation time predicted by new FE simulation

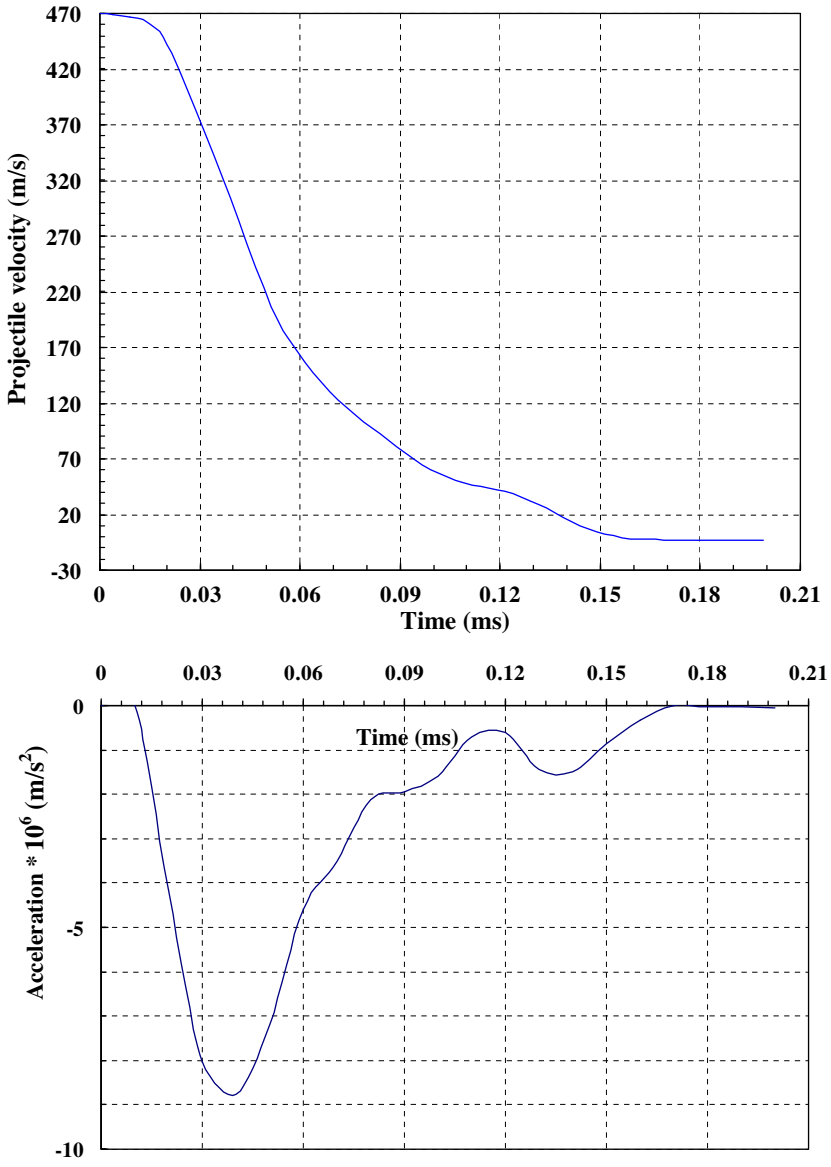

Fig. 7. Velocity and acceleration of projectile during perforation Projectile initial velocity: 470 m/s.

has good consistency with the Chocron–Galvez [10] numerical model.

In Fig. 3, the value of residual velocities computed by FE simulation has been compared with the Chocron–Galvez numerical and analytical [10] models. At the initial impact velocities between 1000 and 1200 m/s, the residual velocities computed by FE simulation have not good agreement with the Chocron–Galvez [10] analytical model and by increasing projectile initial velocity the agreement increases. Also at the initial velocities between 1000 and 1200 m/s, the residual velocities computed by FE simulation have good correlation with the Chocron–Galvez [10] numerical model.

In Fig. 4, the residual velocities computed by FE simulation has been compared with the Feli et al. [13] analytical and Chocron–Galvez [10] numerical models. It is clear that at the initial velocities between 1000 and 1600 m/s the residual velocities computed by LS-Dyna simulation have good agreement with the Chocron–Galvez [10] numerical and Feli et al. [13] analytical models, and in initial velocities greater than 1600 m/s the agreement of the FE simulation and Feli et al. [13] analytical model decreases.

Therefore the residual velocity computed by LS-Dyna FE code presented in this paper at the initial impact velocity between 1000 and 1600 m/s have good correlation with the Chocron–Galvez [10] numerical and Feli et al. [13] analytical models and the results is better than Chocron–Galvez [10] analytical model.

In the new FE simulation presented in this paper the intact and fragmented ceramic material strengths are evaluated from the Johnson–Holmquist's model [17]. Based on the Johnson–Holmquist's model [17] the fragmented ceramics with reduced material strength penetrate into composite or projectile materials. Also the Composite-Damage Model which determined the failure of composite under fiber fracture, matrix cracking or compressive failure has been used for material behavior of composite material. But the strain-rate effect has been ignored in stress–strain relationship of yarns.

3.2. Ceramic/composite performance

In this section the performance of ceramic/composite armor under impact of tungsten projectile has been investigated. The residual velocity versus initial velocity of projectile for the projectile-target system used in this paper has been shown in Fig. 5. From Fig. 5 it is clear that at the initial velocity 470 m/s the residual velocity predicted by LS-Dyna FE code is zero, therefore the ballistic limit velocity of projectile (the minimum velocity of projectile for perforation the ceramic/composite armor) is 470 m/s.

In Table 5, the residual velocities computed by LS-Dyna simulation have been compared with the Chocron–Galvez [10] and Shokrieh and Javadpour [11] numerical models. At the initial velocities between 1100 m/s and 1400 m/s, the good consistency between

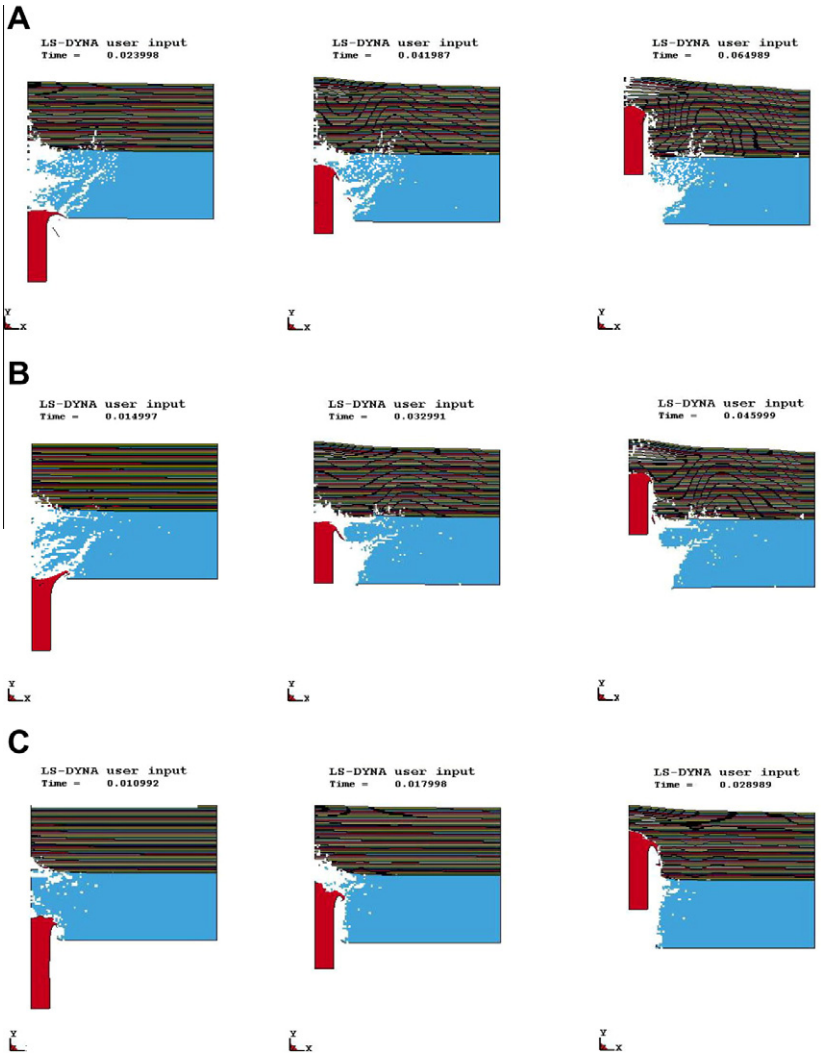

Fig. 8. Projectile, ceramic and composite layers deformation in three projectile initial velocities (A) 900 m/s(B) 1250 m/s (C) 1800 m/s.

results has been observed. Also from Fig. 5 and Table 5, it is clear that near the ballistic limit velocity (between 470 m/s and 500 m/s) there is an incremental jump in the computed residual velocity. The deformation of projectile, ceramic and composite material at initial velocity 470 m/s and 900 m/s has been shown in Fig. 6. As shown in Fig. 6, the perforation time and the dishing of composite material at the initial velocity 470 m/s is greater than 900 m/s. Near the ballistic limit velocity the projectile will remained in the fragmented ceramic tile for more time and the deflection of composite material will be increased. In the initial velocity 900 m/s, the transverse waves have no time to propagation and case the deformation of composite layers. But for impact velocities greater than 500 m/s the composite material layers are broken and perforation time decreases.

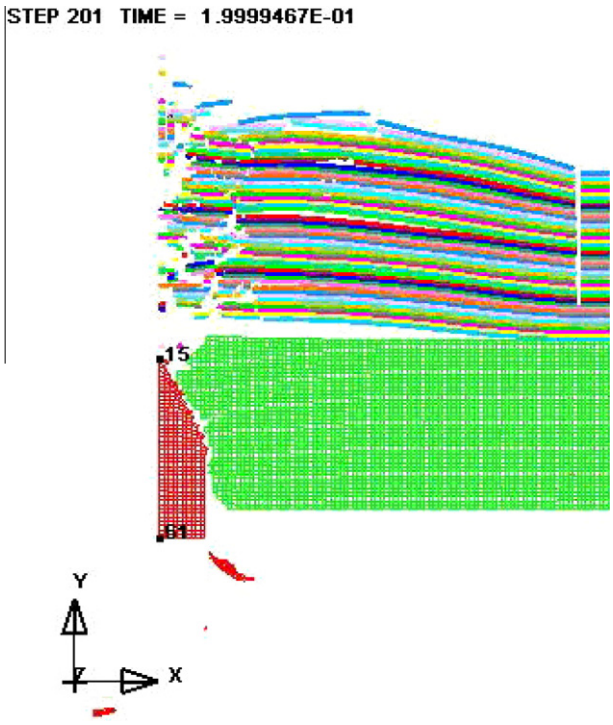

Fig. 9. Erosion of projectile and ceramic during perforation Projectile initial impact velocity 470 m/s perforation time: 200 μs.

The velocity and acceleration of projectile at initial impact velocity 470 m/s has been shown in Fig. 7. The projectile velocity decrease during perforation and perforation time is 200 μs. Near the ballistic limit velocity the deformation of fiber increases and hence the perforation time increases. Also it is clear that upon the impact of projectile on ceramic tile the acceleration of projectile increases and during perforation decreases.

Fig. 8 shows the deformation of projectile, ceramic and composite materials at three different initial impact velocities. Based on the FE simulation, when a ceramic is impacted by a projectile a compressive wave travels from the front to the rear face at the speed of sound, then reflects and becomes a tensile wave which breaks the ceramic in tension, producing in the ceramic tile a conical cracking front advancing in impact direction. Then the projectile starts to penetrate into the fragmented ceramic conoid where the compressive strength has reduced. Depending on the initial impact velocity, there would be three possible situations the tip of the projectile will be flowing or not, also the fragmented ceramic tile may be eroded completely. Finally, the projectile or the projectile and fragmented ceramic conoid case the deflection of composite layers and the remaining kinetic energy of projectile is absorbed by strain and kinetic energy of layers, Based on the failure criteria of composite material the fracture of fibers or matrix may be happened and the projectile perforates the back-up composite.

By considering three initial velocities shown in Fig. 8, it is clear that in the FE simulation with increasing projectile initial velocity, the semi-angle of fragmented ceramic conoid decreases, This result has good agreement with the Wilson and Hetherington [23] experiments and Feli et al. [13] analytical model.

Also based on the LS-Dyna FE simulation results presented in Fig. 8, it has been observed that with increasing projectile initial velocity, the delamination of upper layers of composite plate decreases. At low initial velocities the delamination of layers is considerable but at high impact velocity, (at 1000 m/s or more) the transversal wave has no time to progress before the failure of the fibers and then the energy absorbed by delamination is very smaller than the kinetic and strain energy, absorbed by fibers. In the Chocron–Galvez [10] and Feli et al. [13] analytical models, the energy absorbed by delamination has been ignored.

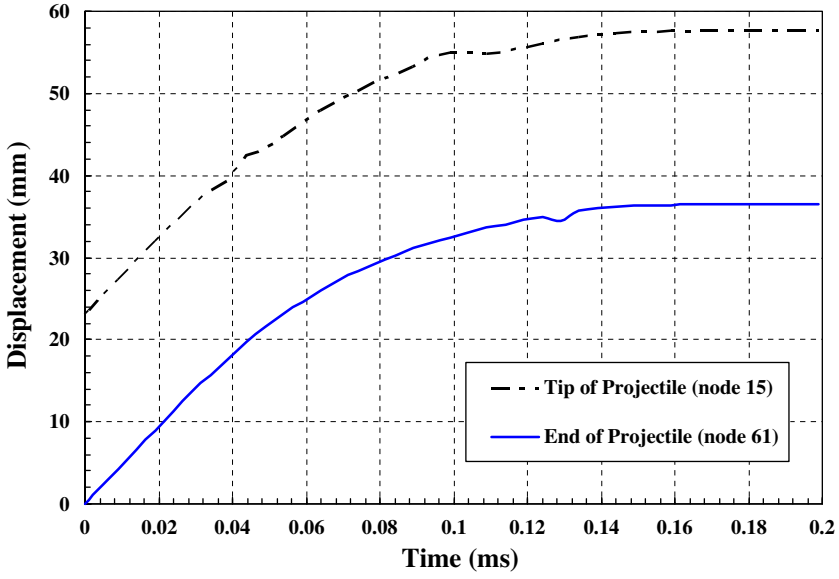

Fig. 10. The displacement of nodes 15 and 61 of projectile during perforation.

The erosion of ceramic and tungsten projectile during perforation has been shown in Fig. 9. The initial velocity of projectile is 471 m/s and perforation time is 200 μs. Based on the FE simulation the projectile tip is eroded and the residual length of projectile is 22.5 mm, therefore 7.5 mm of projectile length is eroded during perforation. The displacement of node 15 on the tip of eroded point of projectile and node 61 at the end projectile (shown in Fig. 9) during perforation has been shown in Fig. 10. It is clear that the total displacement of projectile during 200 μs of perforation is 17 mm, therefore the fragmented ceramic conoid is eroded and the projectile is stopped by composite layers.

The FE simulation technical presented in this paper is the simple and accurate method, which has a good prediction of perforation resistance of ceramic/composite targets. This simulation can be developed for perforation resistance of functionally graded materials (FGM). In this simulation the effects of most important parameters affected the perforation process have been considered. The coefficients of the material behaviors used for the ceramic, composite and projectile have been determined from the other references, determination of those coefficients for the ceramic, composite and projectile materials need the experimental procedure.

4. Conclusions

This paper presents a new technique for FE simulation, based on LS-Dyna code, for high-velocity impact onto the ceramic/composite armor with the total thickness 40 mm. The perforation time computed by the new FE simulation has a good agreement with Chocron–Galvez [10] numerical model. At initial velocities between 1000 and 1600 m/s the residual velocities computed by the FE simulation has an acceptable consistency with the Chocron–Galvez [10] numerical and Feli et al. [13] analytical models. Also the ballistic limit velocity of projectile can be computed by this method. Based on the FE simulation, when the projectile impacted the ceramic front plate a fragmented ceramic conoid breaks from ceramic tile and the semi-angle of ceramic conoid with increasing projectile initial velocity decreases. At the initial velocities between 470 and 500 m/s, an incremental jump in the computed residual velocity of projectile has been observed, near the ballistic limit velocity the projectile will remained in the fragmented ceramic tile for more time and the dishing of composite layers increases, also with increasing projectile initial velocity, the delamination of upper layers of composite plate decreases.

References

[1] Roylance D. Wave propagation in a viscoelastic fiber subjected to transverse impact. ASME J Appl Mech 1973;40:143–8.
[2] Zhu G, Goldsmith W, Dharan CKH. Penetration of laminated Kevlar by projectiles – I. Experimental investigation. Int J Solid Struct 1992;29(4):399–420.
[3] Wen HM. Predicting the penetration and perforation of FRP laminates struck normally by projectiles with different nose shapes. Compos Struct 2000;49:321–9.
[4] Gu B. Analytical modeling for the ballistic perforation of planar plain woven fabric target by projectile. Composites (Part B) 2003;34(4):361–71.
[5] Cottrell MG, Yu J, Owen DRJ. The adaptive and erosive numerical modelling of confined boron carbide subjected to large-scale dynamic loadings with element conversion to undeformable meshless particles. Int J Impact Eng 2003;28:1017–35.
[6] Fawaz Z, Zheng W, Behdinan K. Numerical simulation of normal and oblique ballistic impact on ceramic composite armors. Compos Struct 2004;63:387–95.
[7] Gu B, Xu J. Finite element calculation of 4-step 3-dimensional braided composite under ballistic perforation. Composites (Part B) 2004;35:291–7.
[8] Mamivand M, Liaghat GH. A model for ballistic impact on multi-layer fabric targets. Int J Impact Eng 2010;37(7):806–12.
[9] Sabouri H, Liaghat GH. Comments on the article: "Ballistic impact of GLARE™ fiber–metal laminates. In: Hoo Fatt, Michelle S, Lin, Chunfu, Revilock Jr, Duane M, Hopkins, Dale A, editors. Compos. Struct 2010; 92(2): 600–1. [Compos Struct 2003;61:73–88].
[10] Chocron Benloulo IS, Sanchez Galvez V. A new analytical model to simulate impact onto ceramic/composite armors. Int J Impact Eng 1988;21(6):461–71.
[11] Shokrieh MM, Javadpour GH. Penetration analysis of a projectile in ceramic composite armor. Compos Struct 2008;82(2):269–76.
[12] Hetherington JG. The optimization of two-component composite armours. Int J Impact Eng 1992;12:229–59.
[13] Feli S, Yas MH, Asgari MR. An analytical model for perforation of ceramic/multi-layered planar woven fabric targets by blunt projectiles. Compos Struct 2011;93(2):548–56.
[14] Zaera R, Sanchez-Galvez V. Analytical modeling of normal and oblique ballistic impact on ceramic/metal Lightweight armours. Int J Impact Eng 1998;21(3):133–48.
[15] Johnson GR, Cook WH. Fracture characteristics of three metals subjected to various strains, strain rates, temperatures and pressures. Eng Fract Mech 1985;21(1):31–48.
[16] Hallquist J.O., 2001. LS-DYNA keywords user's manual-Volume II (version 960), Livermore software technology corp. Livermore.
[17] Johnson GR, Holmquist TJ. An improved computational constitutive model for brittle materials. High pressure science & technology. New York: AIP Press; 1994. pp. 981–984.
[18] Cronin Duane S, Khahn Bui, Christian Kaufmann, Grant Mclntosh, Todd Berstad. Implementation and validation of the johnson–holmquist-ceramic material model in LS-DYNA, 4th European LS-DYNA users conference, material I, Germany; 2003.
[19] Chamis CC. NASA tech. Memo 83320. (presented at the 38th annual conference of the society of plastics industry (SPI), Houston, TX; February, 1983.
[20] Zhang GM, Batra RC, Zheng J. Effect of frame size, frame type, and clamping pressure on the ballistic performance of soft body armor. Composites (Part B) 2008;39:476–89.
[21] Lim CT, Ng YH, Shim VPW. Finite element modeling of the ballistic impact into fabric armor. Int J Impact Eng 2003;28(1):13–31.
[22] Cheeseman BryanA, Travis Bogetti A. Ballistic impact into fabric and compliant composite laminates. Compos Struct 2003;61:161–73.
[23] Wilson D., J. G. Hetherington, Analysis of ballistic impact on ceramic faced armour using high speed photography. Proc. lightweight armour system symp., Royal Military College of Science, Cranfield; 1995.